SUPPLEMENTAL FIGURES AND TABLES

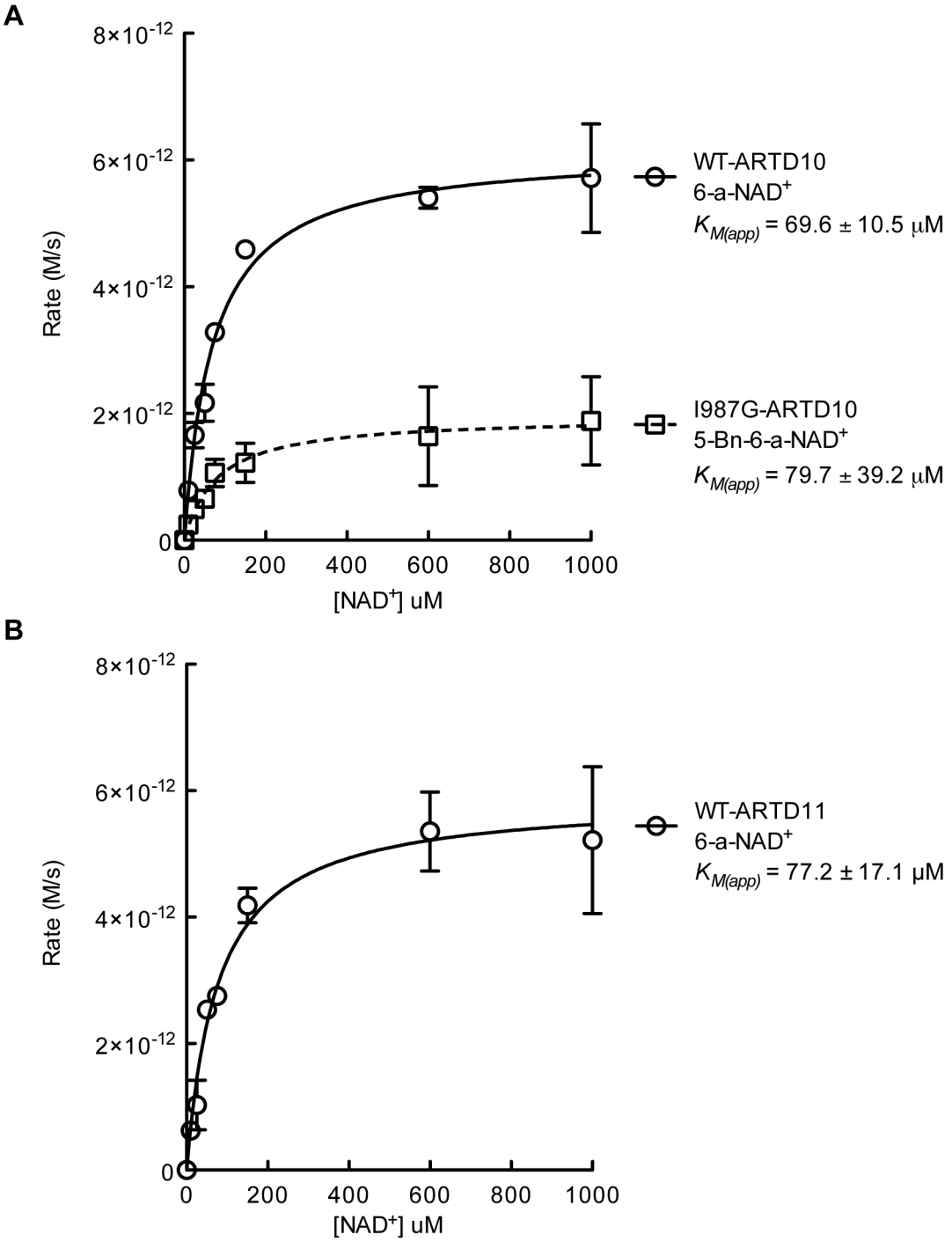

Figure S1. Kinetic Analysis of *in vitro* ARTD$_{cat}$ Activity, Related to Figures 1-3. (**A**) The initial rate of SRPK2 MARylation by either WT-ARTD10 (circles) or IG-ARTD10 (squares) is plotted against the concentration of 6-a-NAD$^+$ (circles) or 5-Bn-6-a-NAD$^+$ (squares). The initial rates were measured in duplicate and $K_{M(app)}$ was determined using the Michaelis-Menten equation. (**B**) The initial rate of SRPK2 MARylation by WT-ARTD11 was determined with varying concentrations of 6-a-NAD$^+$ as in A.

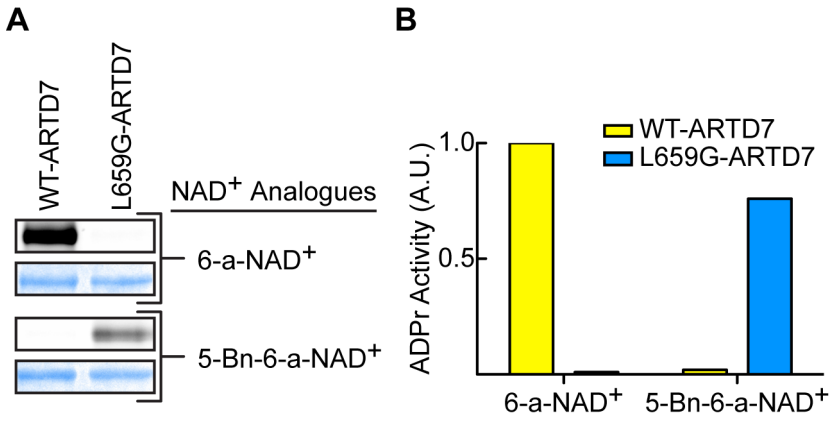

Figure S2. LG-ARTD7 Uses 5-Bn-6-a-NAD$^+$ as an Orthogonal Substrate, Related to Figure 1. (A) Results from orthogonal MARylation of SRPK2 by LG-ARTD7 and 5-Bn-6-a-NAD$^+$. WT- and LG-ARTD7 are indicated above the gel and the non-substituted 6-a-NAD$^+$ and 5-Bn-6-a-NAD$^+$ probes are listed to the right of the gel. For each modified NAD$^+$ analogue tested the same gel was first fluorescently imaged to detect SRPK2 MARylation (top gel, gray) and then stained to detect total SRPK2 (bottom gel, blue). (B) Quantification of the results from (A).

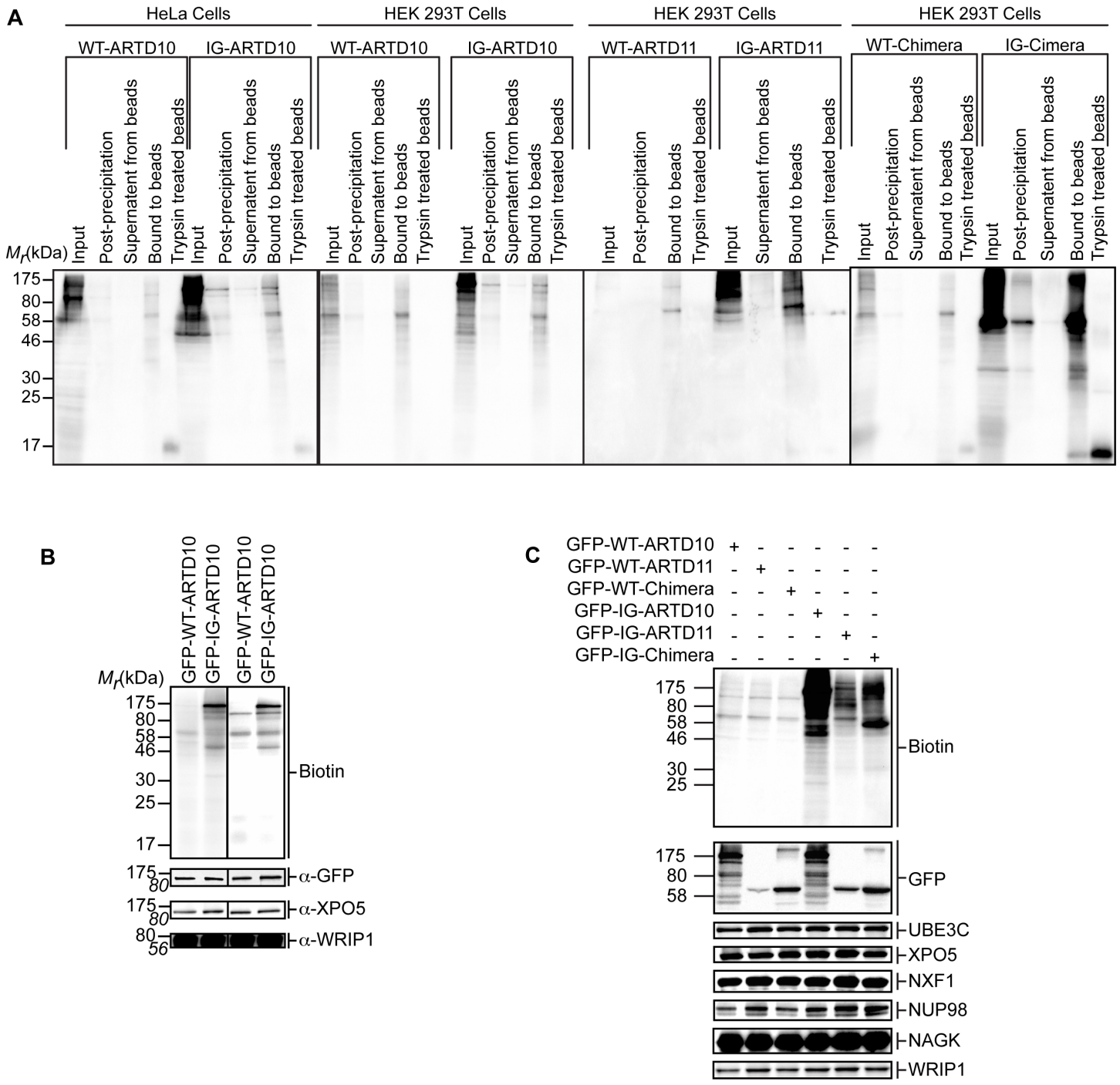

Figure S3. Immunoblot Verification of the LC-MS/MS Preparation and Input Controls for LC-MS/MS Target Validation, Related to Figures 2-4 and Tables S1-S3 and S4. (A) The indicated fractions from the NeutrAvidin enrichment protocol (Carter-O'Connell et al., 2015) were imaged using streptavidin-HRP. 5-Bn-6-a-NAD^+ was spiked into the appropriate lysate (expressing either WT- or IG-ARTD), samples were labeled, conjugated to biotin-PEG_3-azide, enriched, and submitted for LC-MS/MS analysis. (B) Immunoblot detection of the input fractions prior to enrichment in Figure 2D. Overall MARylation levels were determined using streptavidin-HRP (Biotin). Differences in labeling efficiency between HEK 293T and HeLa lysate required separate immunoblot exposures. (C) As in (B) for Figure 4C.

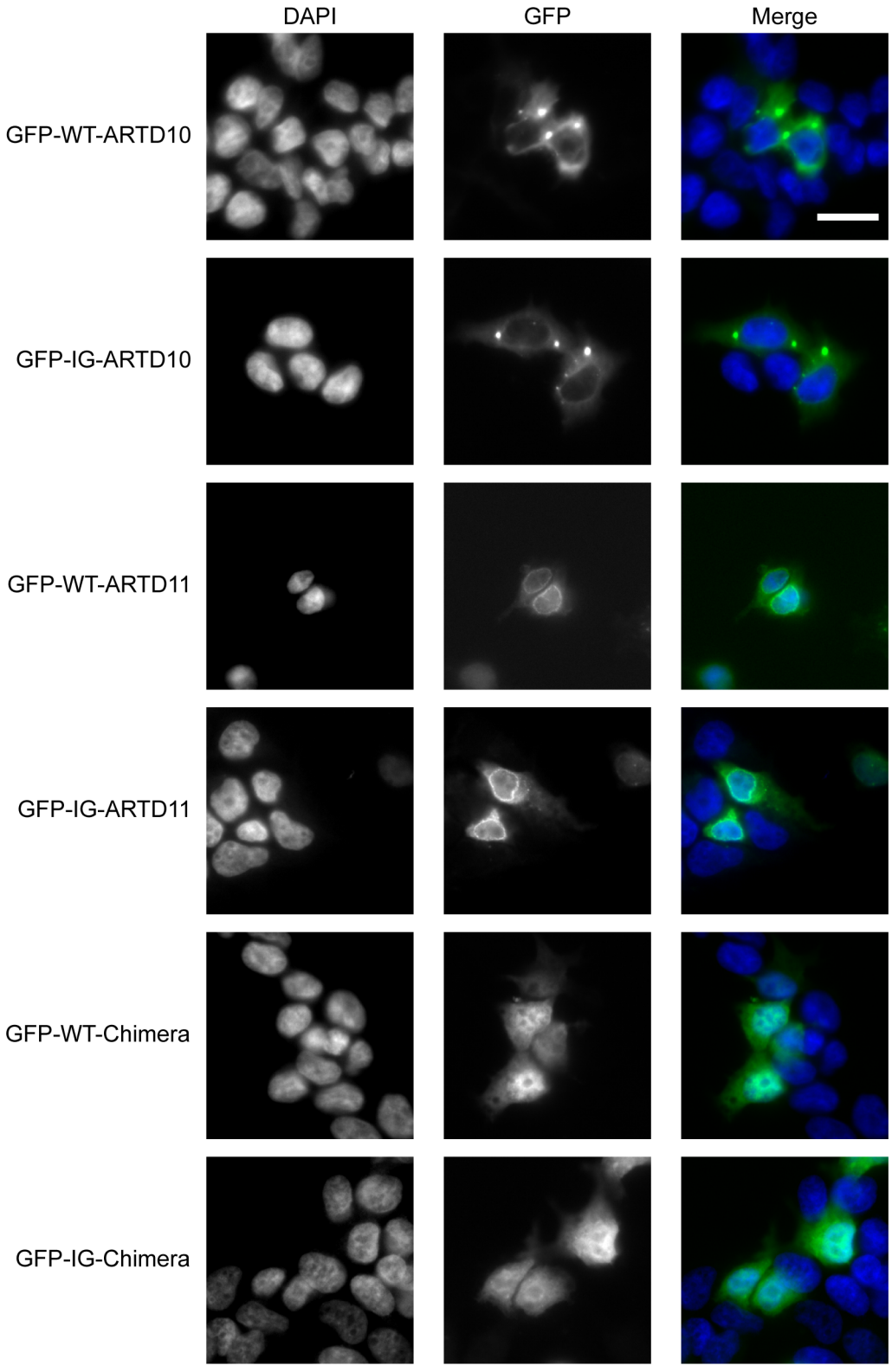

Figure S4. Differences in Cellular Localization Between mono-ARTD Family Members, Related to Figure 5. HEK 293T cells expressing GFP-tagged variants of either WT- or IG-ARTD10, -ARTD11, or -Chimera were fixed with paraformaldehyde and processed for GFP-fluorescence. DNA was stained with DAPI. The IG variants maintain the same cellular localization as their WT counterparts. Scale bar = 20 μm.

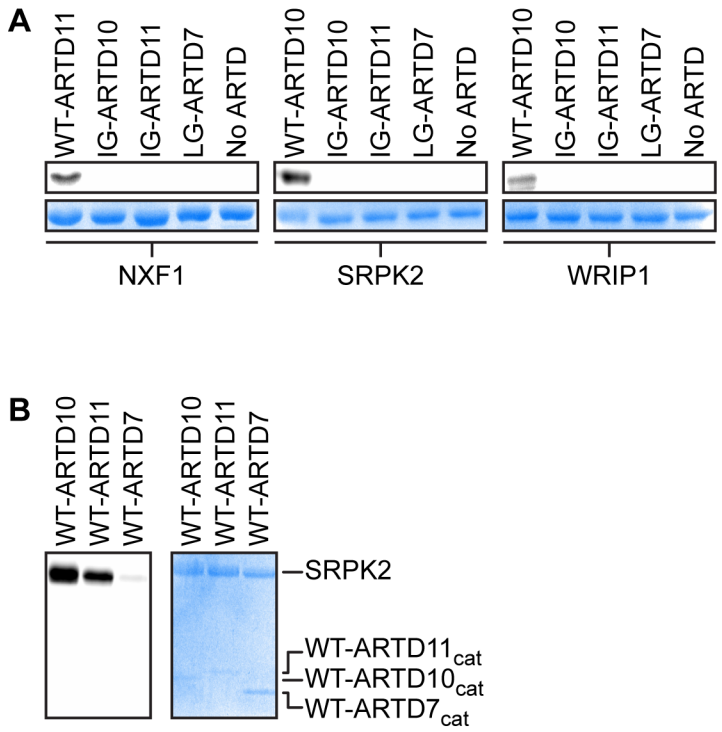

Figure S5. Selective MARylation of NXF1, SRPK2, and WRIP1 Requires an Active ARTD and is not Limited by Auto-MARylation, Related to Figure 5. (A) *In vitro* IG/LG-ARTD$_{cat}$ MARylation assays demonstrate that an active ARTD is required for ADP-ribose transfer. IG-ARTD10$_{cat}$, -ARTD11$_{cat}$, and LG-ARTD7$_{cat}$ were screened for MARylation activity using recombinant NXF1, SRPK2, and WRIP1 in the presence of 6-a-NAD^{+}. The preferred WT-ARTD is included as a positive control. The same gel was first fluorescently imaged to detect substrate MARylation (top gel, gray) and then stained to detect total substrate (bottom gel, blue). (B) WT-ARTD$_{cat}$ proteins are not auto-MARylated *in vitro*. WT-ARTD10$_{cat}$, -ARTD11$_{cat}$, and -ARTD7$_{cat}$ were screened for MARylation activity in the presence of 6-a-NAD^{+}. SRPK2 was included as a positive MARylation control. The same gel was first fluorescently imaged to detect substrate MARylation (left gel, gray) and then stained to detect total substrate (right gel, blue).

Table S1. LC-MS/MS Results from HEK 293T Lysate Labeling with IG-ARTD10 and 5-Bn-6-NAD$^+$, Related to Figures 2-4. [a]Accesion ID and description from the UniProt reference proteome set: www.uniprot.org/taxonomy/9606. ARTD10 targets that pass thresholds in duplicate are indicated in bold. Targets are colored based on their identification frequency in the pooled background data sets (white: < 3, light blue: <6, dark blue ≥ 9). [b]Total counts are the combined values for unique peptides and the adjusted fraction of shared peptides. [c]HeLa targets are identified in Table S2 (--: absent in HeLa set, +: present in HeLa set). [d]ARTD1 and ARTD2 targets were identified previously (Carter-O'Connell et al., 2014) (--: absent in ARTD1/2 set, +: present in ARTD1/2 set). [e]ARTD11 targets are identified in Table S3 (--: absent in ARTD11 set, +: present in ARTD11 set, ++: present in ARTD11 set in duplicate). [f]Chimeric targets are identified in Table S4 (--: absent in chimera set, +: present in chimera set).

Table S2. LC-MS/MS Results from HeLa Lysate Labeling with IG-ARTD10 and 5-Bn-6-NAD$^+$, Related to Figure 2. [a]Accesion ID and description from the UniProt reference proteome set: www.uniprot.org/taxonomy/9606. ARTD10 targets that pass thresholds in duplicate are indicated in bold. Targets are colored based on their identification frequency in the pooled background data sets (white: < 3, light blue: <6, dark blue ≥ 9). [b]Total counts are the combined values for unique peptides and the adjusted fraction of shared peptides. [c]HEK 293T targets are identified in Table S1 (--: absent in HEK 293T set, +: present in HEK293T set, ++: present in HEK 293T set in duplicate). [d]ARTD1 and ARTD2 targets were identified previously (Carter-O'Connell et al., 2014) (--: absent in ARTD1/2 set, +: present in ARTD1/2 set). [e]ARTD11 targets are identified in Table S3 (--: absent in ARTD11 set, +: present in ARTD11 set).

Table S3. LC-MS/MS Results from HEK 293T Labeling with IG-ARTD11 and 5-Bn-6-NAD$^+$, Related to Figures 3-4. [a]Accesion ID and description from the UniProt reference proteome set: www.uniprot.org/taxonomy/9606. ARTD11 targets that pass thresholds in duplicate are indicated in bold. Targets are colored based on their identification frequency in the pooled background data sets (white: < 3, light blue: <6, dark blue ≥ 9). [b]Total counts are the combined values for unique peptides and the adjusted fraction of shared peptides. [c]ARTD1 and ARTD2 targets were identified previously (Carter-O'Connell et al., 2014) (--: absent in ARTD1/2 set, +: present in ARTD1/2 set). [d]ARTD10 targets are identified in Table S1 (--: absent in ARTD10 set, +: present in ARTD10 set, ++: present in ARTD10 set in duplicate). [e]Chimeric targets are identified in Table S4 (--: absent in chimera set, +: present in chimera set).

Table S4. GO Term Enrichment and Term Condensation for ARTD10 or ARTD11 Specific Protein Targets, Related to Figure 3. [a]GO IDs and GO biological processes for significantly enriched terms ($p<0.05$) were identified using Amigo 2 version 2.2.0 (Ashburner et al., 2000), using the monthly release of June 2015. [b]Uniqueness is determined based on the likelihood that the GO term is an outlier when compared to the entire list. Calculated as 1-(average semantic similarity of the term to all other terms). [c]The semantic similarity threshold at which the term would be removed and assigned to a cluster. For the present analysis, the dispensability threshold was set to 0.40).

Table S5. LC-MS/MS Results from HEK 293T Labeling with IG-chimera and 5-Bn-6-NAD$^+$, Related to Figure 4. [a]Accesion ID and description from the UniProt reference proteome set: www.uniprot.org/taxonomy/9606. Chimera targets that pass thresholds in duplicate are indicated in bold. Targets are colored based on their identification frequency in the pooled background data sets (white: < 3, light blue: <6, dark blue ≥ 9). [b]Total counts are the combined values for unique peptides and the adjusted fraction of shared peptides. [c]ARTD10 targets are identified in Table S1 (--: absent in ARTD10 set, +: present in ARTD10 set, ++: present in ARTD10 set in duplicate). [d]ARTD11 targets are identified in Table S3 (--: absent in ARTD11 set, +: present in ARTD11 set, ++: present in ARTD11 set in duplicate).

Table S6. ARTD10 and ARTD11 Specific Protein Targets Identified in Previous ADP-Ribosyl Proteome Studies, Related to Figure 5 and Tables S1 and S3. [a]Accesion ID and description from the UniProt reference proteome set: www.uniprot.org/taxonomy/9606. [b]ARTD1 and ARTD2 targets were identified previously (Carter-O'Connell et al., 2014) (--: absent in ARTD1/2 set, +: present in ARTD1/2 set). [c]ARTD10 targets are identified in Table S1 (--: absent in ARTD10 set, +: present in ARTD10 set, ++: present in ARTD10 set in duplicate). [d]ARTD11 targets are identified in Table S3 (--: absent in ARTD11 set, +: present in ARTD11 set, ++: present in ARTD11 set in duplicate). [e]Previously identified ARTD targets are annotated with the appropriate reference.

SUPPLEMENTAL EXPERIMENTAL PROCEDURES

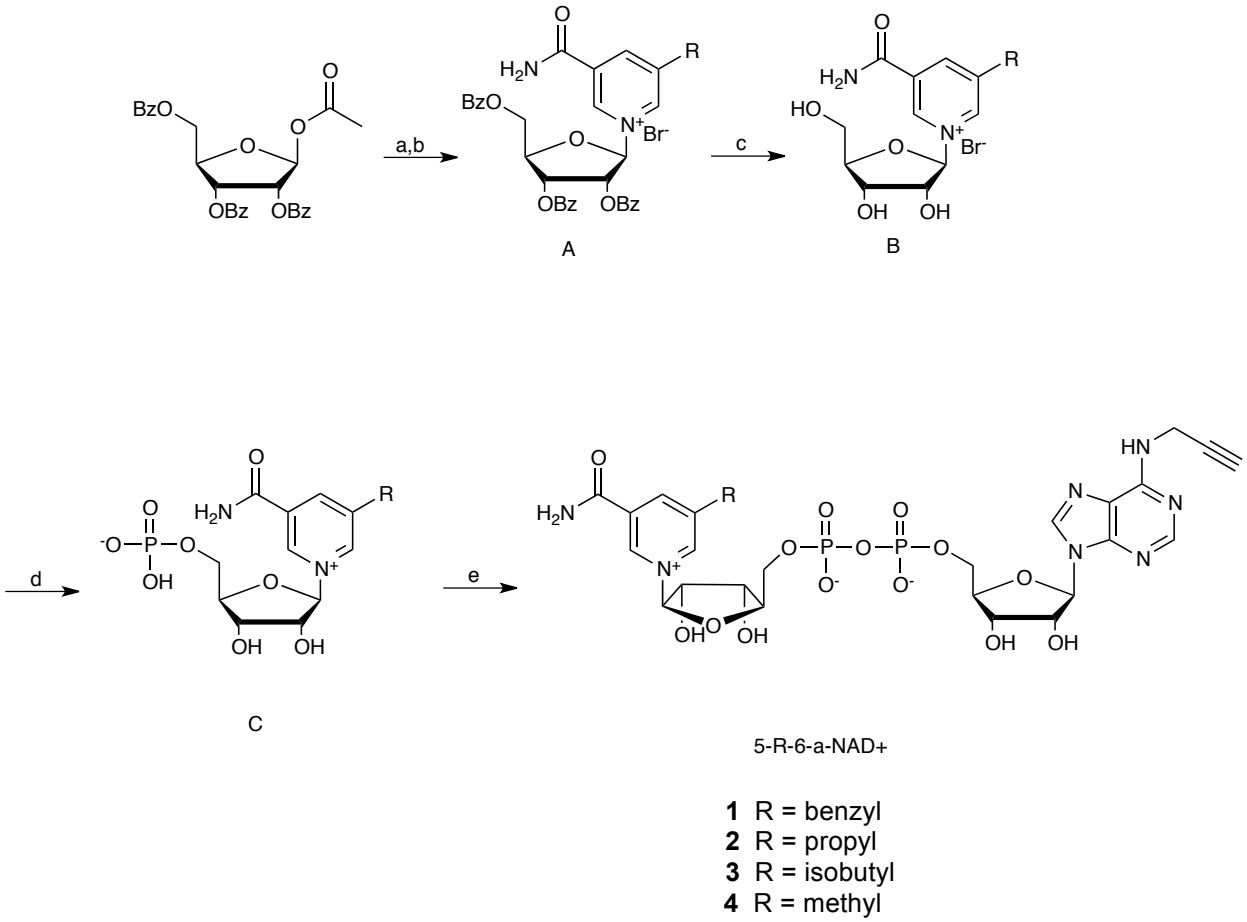

1 R = benzyl
2 R = propyl
3 R = isobutyl
4 R = methyl

Scheme S1. Synthesis of C-5 substituted 6-a-NAD$^+$ analogues, Related to Figure 1. Reagents and conditions: (a) HBr (33 wt% in acetic acid), toluene, 0 ^oC; (b) C-5 substituted nicotinamide, MeCN; (c) 7N NH_3 in MeOH, -10 ^oC; (d) $POCl_3$, trimethyl phosphate, H_2O, rt; (e) 6-allkyne-AMP-morpholidate, $MnCl_2$, $MgSO_4$, formamide, rt.

General Synthesis. ^1H and ^{13}C NMR were recorded on a Bruker DPX spectrometer at 400 MHz and 100 MHz, respectively. Chemical shifts are reported as parts per million (ppm) downfield from an internal tetramethylsilane standard or solvent references. For air- and water-sensitive reactions, glassware was oven-dried prior to use and reactions were performed under argon. Dichloromethane, dimethylformamide, and tetrahydrofuran were dried using the solvent purification system manufactured by Glass Contour, Inc. (Laguna Beach, CA). All other solvents were of ACS chemical grade (Fisher Scientific) and used without further purification unless otherwise indicated. Commercially available starting reagents were used without further purification. Nicotinamide (Sigma-Aldrich, >99.5%), and 5-methylnicotinamide (Alfa Aesar, 97%) were used without further purification. Analytical thin-layer chromatography was performed with silica gel 60 F_{254} glass plates (SiliCycle). Flash column chromatography was conducted with either pre-packed Redisep R_f normal/reverse phase columns (Teledyne ISCO) or self-packed columns containing 200-400 mesh silica gel (SiliCycle) on a Combiflash Companion purification system (Teledyne ISCO). High performance liquid chromatography (HPLC) was performed on a Varian Prostar 210 (Agilent) with a flow rate of 20 ml/min using Polaris 5 C18-A columns (150 x 4.6 mm, 3 mm - analytical, 150 x 21.2 mm, 5 mm-preparative) (Agilent). UV-Vis detection: λ_1 = 254 nm, λ_2 = 280 nm.

General procedure for the synthesis of N'-(2,3,5-Tri-O-Benzoyl-b-D-ribofuranosyl)-3-aminocarbonyl-5-R-pyridinium bromide A. b-D-ribofuranose-acetate-2, 3, 5-tribenzoate (504 mg, 1 mmol) was dissolved in toluene (15 ml) and cooled to 0°C. HBr (33 wt% in acetic acid) (368 mg, 1.5 mmol) was added dropwise and the reaction was stirred at 0°C for 2 h. 0.5 ml of the solution mixture was taken and evaporated to dryness for ^1H NMR analysis [chemical shifts for the anomeric protons: b isomer = 6.6 ppm (s, 1H); a isomer = 6.9 ppm (d, 1H)]. After the starting material was consumed and ^1H NMR confirmed the formation of the b isomer, the reaction was concentrated in vacuo. The crude b-D-ribofuranose-bromo-2, 3, 5-tribenzoate was azeotroped with toluene (3 x 20 ml) to remove remaining acetic acid and dried in vacuo for 2 h. Crude b-D-ribofuranose-bromo-2, 3, 5-tribenzoate and appropriate C-5-substituted nicotinamide (90 mg, 0.55 mmol) (prepared as described previously: Carter-O'Connell et al., 2014) was dissolved in ACN (40 ml). The reaction was stirred under Ar gas at rt for 2 days. The reaction was concentrated *in vacuo* (temperature kept below 35°C). The crude product was dissolved in $CHCl_3$ (2 ml) and ppt by adding ethyl ether (10 ml). The entire procedure was repeated three times to yield the desired product, which was used in subsequent reactions without further purification.
1A: yield, 260 mg (58%)
2A: yield, 350 mg (92%)

3A: yield, 230 mg (60%)
4A: yield, 282 mg (77%)

General procedure for the synthesis of N'-(b-D-ribofuranosyl)-3-aminocarbonyl-5-R-pyridinium bromide B. **A** was dissolved in ammonia (25 ml, 7 N in MeOH) and the reaction was stirred at -10°C for 36 h. The reaction was concentrated *in vacuo* and the crude product was dissolved in MeOH (1 ml). Addition of ethyl ether 10 ml) resulted in ppt of the desired product. The procedure was repeated three times to yield the desired product as an off white powder (90 mg, 66% yield), which was used in subsequent reactions without further purification. Some epimerization was observed (~5-10% a isomer was present as determined by ^{1}H NMR analysis).

1B: amount of **1A**: 100 mg, 0.14 mmol; yield, 35 mg (60%). ^{1}H NMR (400 MHz, D_2O) δ 9.42 (s, 1H), 9.08 (s, 1H), 8.78 (d, J = 1.7 Hz, 1H), 7.49 – 7.25 (m, 5H), 6.16 (d, J = 4.1 Hz, 1H), 4.42 (dd, J = 6.0, 3.4 Hz, 2H), 4.36 – 4.22 (m, 3H), 3.98 (dd, J = 13.0, 2.9 Hz, 1H), 3.81 (dd, J = 13.0, 3.5 Hz, 1H).
2B: amount of **2A**: 250 mg, 0.36 mmol; yield, 90 mg (66%). ^{1}H NMR (400 MHz, D_2O) δ 9.40 (s, 1H), 9.13 (s, 1H), 8.81 (s, 1H), 6.19 (d, J = 4.2, 1H), 4.45 (m, 2H), 4.33 (m, 1H), 4.05 (ddd, J = 13.0, 2.8, 1.7 Hz, 1H), 3.88 (ddd, J = 12.9, 3.3, 1.7 Hz, 1H), 2.97 (t, J = 7.5 Hz, 2H), 1.73 (q, J = 7.5 Hz, 2H), 0.92 (t, J = 7.5, 3H).
3B: amount of **3A**: 140 mg, 0.20 mmol; yield, 62 mg (79%). ^{1}H NMR (400 MHz, D_2O) δ 9.41 (s, 1H), 9.14 (s, 1H), 8.79 (s, 1H), 6.19 (d, *J* = 4.2 Hz, 1H), 4.45 (t, *J* = 4.3 Hz, 2H), 4.33 (d, *J* = 5.1 Hz, 1H), 4.05 (d, *J* = 13.2 Hz, 1H), 3.89 (d, *J* = 12.9 Hz, 1H), 2.81 (d, *J* = 7.2 Hz, 2H), 2.07 – 1.90 (m, 1H), 0.91 (d, *J* = 6.6 Hz, 6H).
4B: amount of **4A**: 140 mg, 0.20 mmol; yield, 71 mg (56%).

General procedure for the synthesis of 5-R-nicotinamide mononucleotide C. **B** was dissolved in trimethyl phosphate (0.18 ml) and the reaction was cooled to 0°C. $POCl_3$ (10 eq.) was added and the reaction was stirred at 0°C for 4 h. A few drops H_2O was then added to quench the reaction. Trimethyl phosphate was removed by extraction with ethyl ether (20 ml). The remaining trimethyl phosphate was removed by a second extraction with THF (5 ml). The aqueous layer was concentrated *in vacuo*. The crude product was dissolved in H_2O (0.5 ml) and purified via two-step ion exchange chromatography (Dowex resin 1 x 2, formate resin, eluted with water; H^+ resin, eluted with water). Fractions containing the desired product were pooled and concentrated *in vacuo* to yield the desired product (54 mg, 60% yield).

1C: amount of **1B**: 30 mg (0.07 mmol); yield, 24 mg (80%). ^{1}H NMR (400 MHz, D_2O) δ 9.28 (s, 1H), 9.03 (s, 1H), 8.70 (s, 1H), 7.30 (d, *J* = 7.6 Hz, 5H), 6.13 – 6.03 (m, 1H), 4.57 (s, 1H), 4.48 (d, *J* = 4.4 Hz, 1H), 4.42 – 4.34 (m, 1H), 4.31 (s, 2H), 4.29 – 4.15 (m, 1H), 4.08 (d, *J* = 11.6 Hz, 1H).
2C: amount of **2B**: 90 mg, 0.24 mmol; yield, 54 mg (60%).^{1}H NMR (400 MHz, D_2O) δ 9.40 (s, 1H), 9.13 (s, 1H), 8.81 (s, 1H), 6.19 (d, *J* = 4.2, 1H), 4.45 (m, 2H), 4.33 (m, 1H), 4.05 (ddd, *J* = 13.0, 2.8, 1.7 Hz, 1H), 3.88 (ddd, *J* = 12.9, 3.3, 1.7 Hz, 1H), 2.97 (t, *J* = 7.5 Hz, 2H), 1.73 (q, *J* = 7.5 Hz, 2H), 0.92 (t, *J* = 7.5, 3H).
3C: amount of **3B**: 100 mg, 0.3 mmol; yield, 74 mg (74%). ^{1}H NMR (400 MHz, D_2O) δ 9.35 (s, 1H), 9.01 (s, 1H), 8.80 (d, *J* = 1.7 Hz, 1H), 6.13 (d, *J* = 5.8 Hz, 1H), 4.61 (d, *J* = 2.4 Hz, 1H), 4.52 (t, *J* = 5.4 Hz, 1H), 4.43 (dd, *J* = 5.0, 2.2 Hz, 1H), 4.34 – 4.19 (m, 1H), 4.18 – 4.05 (m, 1H), 2.83 (d, *J* = 7.2 Hz, 2H), 2.00 (m, 1H), 0.91 (dd, *J* = 6.6, 4.9 Hz 6H).
4C: amount of **4B**: 60 mg, 0.17 mmol; yield, 22 mg (37%). ^{1}H NMR (400 MHz, D_2O) δ 9.23 (s, 1H), 9.07 (s, 1H), 8.76 (s, 1H), 6.11 (dd, *J* = 5.6, 2.4 Hz, 1H), 4.58 (p, *J* = 2.5 Hz, 1H), 4.50 (td, *J* = 5.2, 2.5 Hz, 1H), 4.40 (dt, *J* = 5.3, 2.7 Hz, 1H), 4.27 (ddd, *J* = 11.8, 4.5, 2.5 Hz, 1H), 4.16 – 3.99 (m, 1H), 2.60 (s, 3H).

General procedure for the synthesis of 5-R-6-a-NAD$^+$ analogues. The appropriate C-5-substituted nicotinamide mononucleotide **C**, 6-alkyne-AMP-morpholidate (1 eq.) (prepared as described previously: Carter-O'Connell et al., 2014), and $MgSO_4$ (16 mg) were dissolved in a solution of $MnCl_2$ (0.5 ml, 0.2 M in formamide) and stirred at rt for 48 h. The reaction was concentrated *in vacuo* and the crude product was purified via preparative HPLC (MP A: 0.1% formic acid (aq), MP B: 0.1% formic acid in ACN; 0-5 min: 0-10%B, 5-8 min: 10-15%B, 8-10 min: 15-20%B, 10-12 min: 20-50%B). Fractions containing the desired product were pooled and concentrated *in vacuo* to yield the desired product.

5-benzyl-6-a-NAD$^+$: amount of **1C**: 11 mg (0.02 mmol); yield, 5 mg (32%). ^{1}H NMR (400 MHz, D_2O) δ 9.11 (s, 1H), 8.98 (s, 1H), 8.55 (s, 1H), 8.37 (s, 1H), 8.14 (s, 1H), 7.41 – 7.09 (m, 5H), 5.96 (t, *J* = 5.0 Hz, 2H), 4.74 – 4.57 (m, 7H), 4.55 – 4.35 (m, 3H), 4.35 – 4.08 (m, 5H), 2.58 (s, 1H).
5-propyl-6-a-NAD$^+$: amount of **2C**: 24 mg (0.05 mmol); yield, 10 mg (27%). ^{1}H NMR (400 MHz, D_2O) δ 9.18 (s, 1H), 8.94 (s, 1H), 8.74 (s, 1H), 8.51 (s, 1H), 8.31 (s, 1H), 6.04 (dd, *J* = 17.2, 5.6 Hz, 2H), 4.72 (m, 1H), 4.60 – 4.28 (m, 6H), 4.29 – 4.09 (m, 3H), 2.86 (t, *J* = 7.6 Hz, 2H), 2.70(s, 1H) 1.68 (dt, *J* = 14.5, 7.2 Hz, 2H), 0.91 (t, *J* = 7.3 Hz, 3H).
5-isobutyl-6-a-NAD$^+$: amount of **3C**: 10 mg (0.02 mmol); yield, 8.9 mg (56%). ^{1}H NMR (400 MHz, D_2O) δ 9.24 (s, 1H), 8.94 (s, 1H), 8.80 – 8.69 (m, 1H), 8.61 – 8.49 (m, 1H), 8.34 (s, 1H), 6.07 (dd, *J* = 16.4, 5.4 Hz, 2H), 4.72 (dd, *J* = 6.6, 4.1 Hz, 1H), 4.65 – 4.30 (m, 4H), 4.24 (d, *J* = 14.9 Hz, 3H), 2.78 (d, *J* = 6.9 Hz, 2H), 2.71(s, 1H), 1.96 (dd, *J* = 13.6, 6.8 Hz, 1H), 0.88 (dd, *J* = 6.5, 4.3 Hz, 6H).
5-methyl-6-a-NAD$^+$: amount of **4C**: 26 mg (0.05 mmol); yield, 9 mg (25%). ^{1}H NMR (400 MHz, D_2O) δ 9.08 (s, 1H), 8.91 (s, 1H), 8.65 (s, 1H), 8.44 (s, 1H), 8.17 (s, 1H), 5.97 (dd, *J* = 18.7, 5.6 Hz, 2H), 4.70 – 4.56 (m, 1H), 4.53 – 4.24 (m, 5H), 4.24 – 4.00 (m, 4H), 2.55 (s, 3H).

^{1}H NMR spectra:

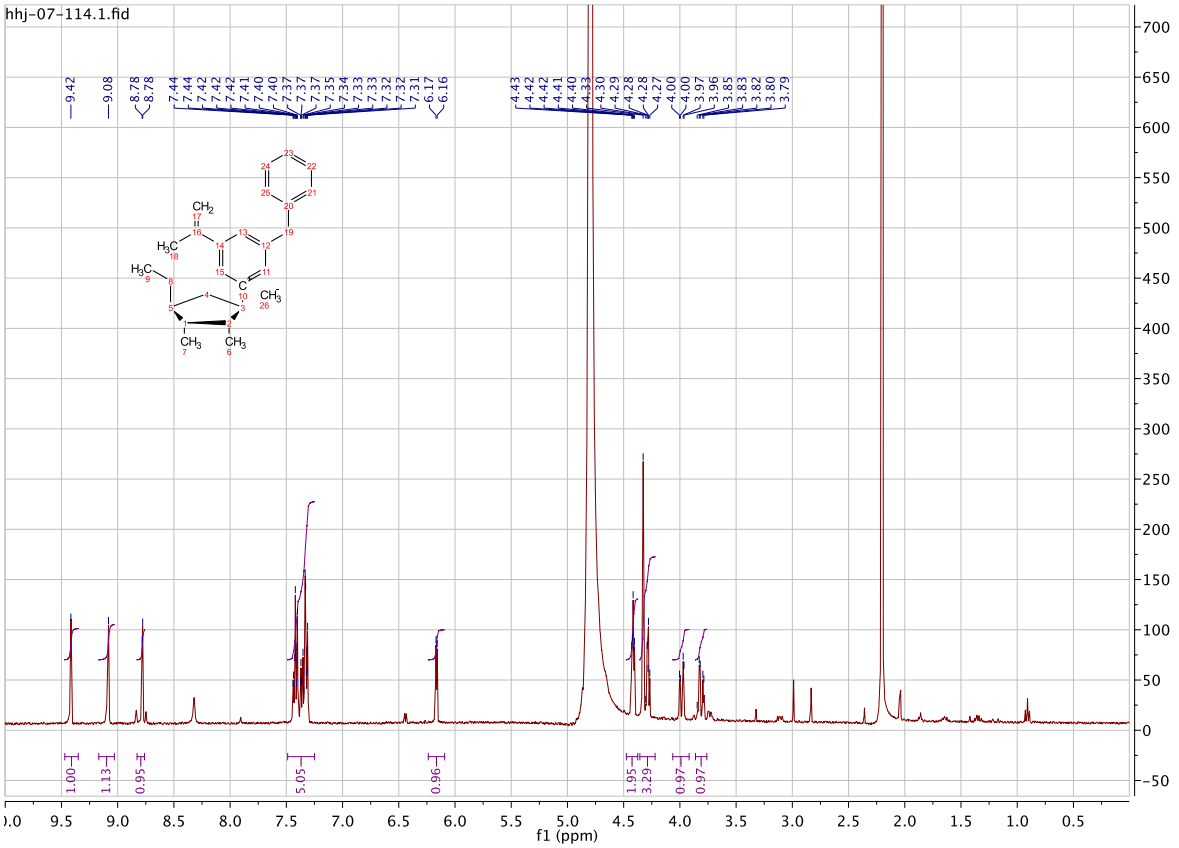

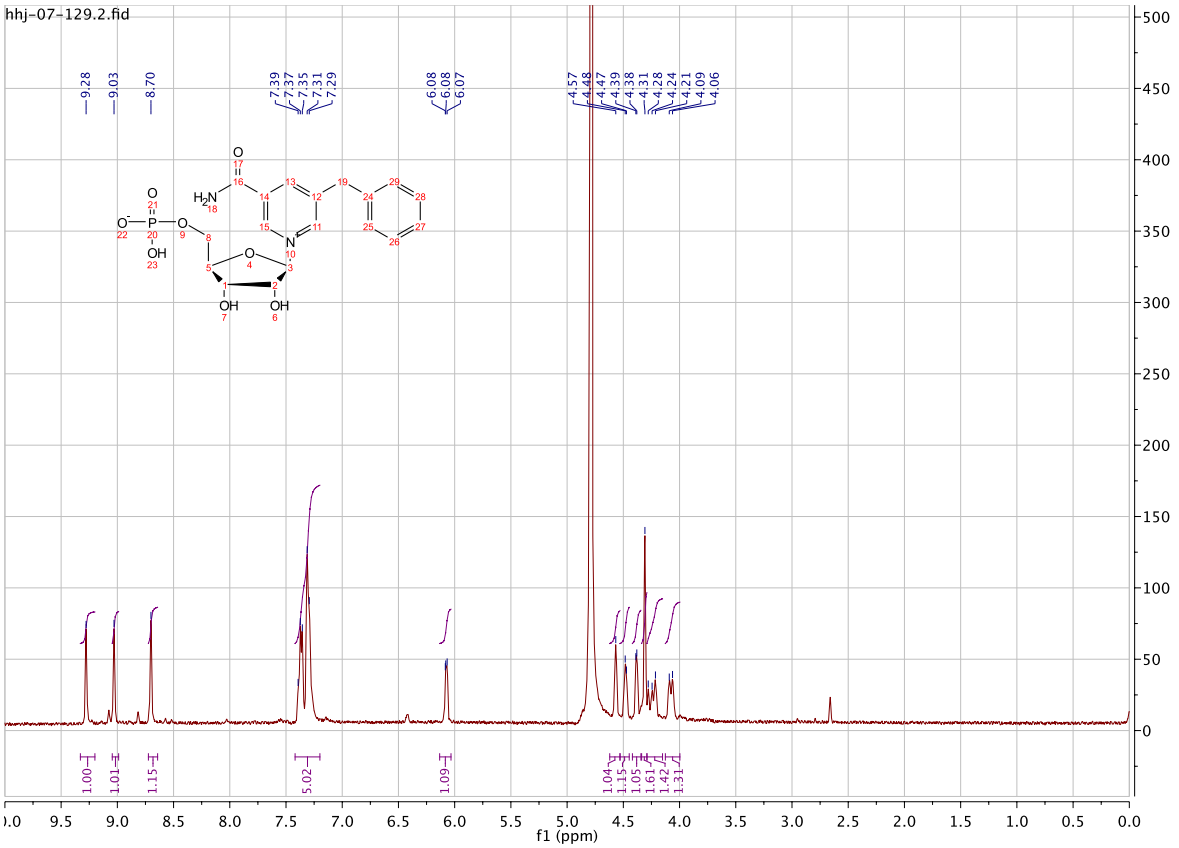

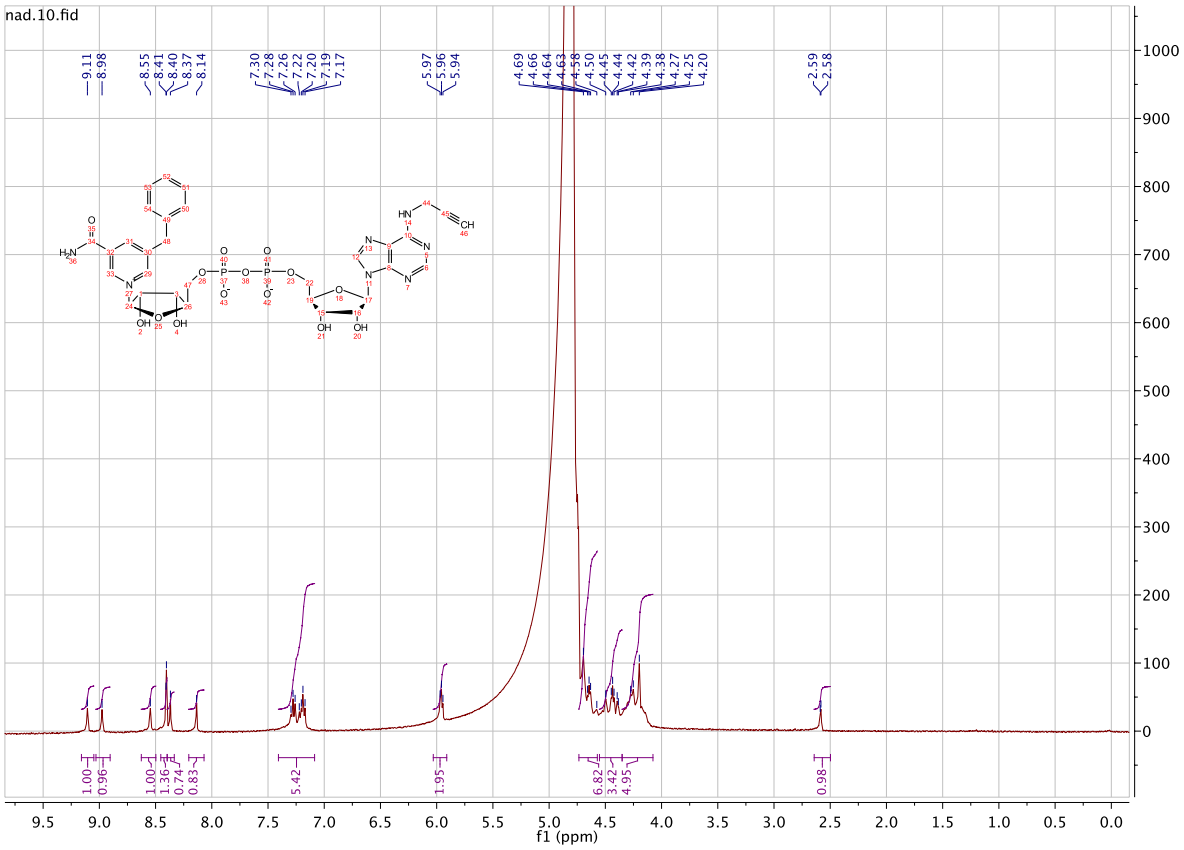
nad.10.fid
f1 (ppm)

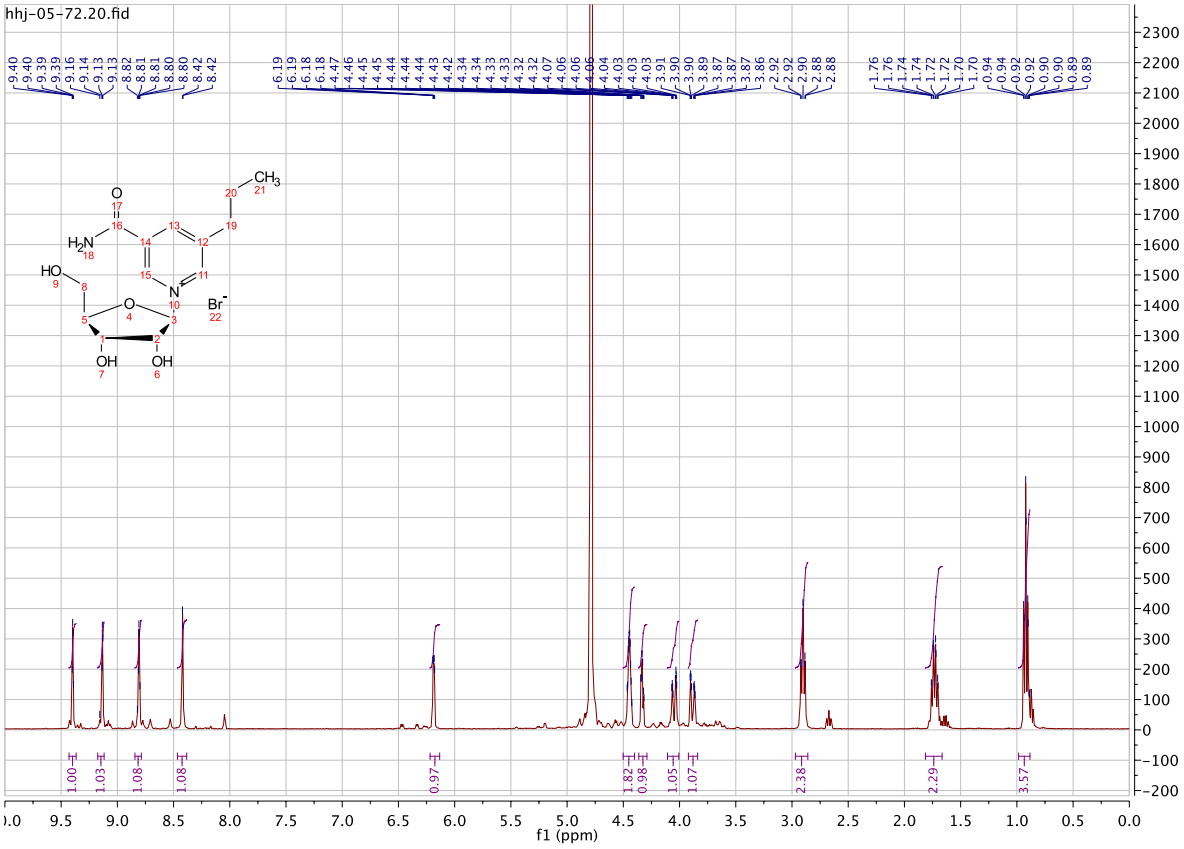
hhj-05-72.20.fid
f1 (ppm)

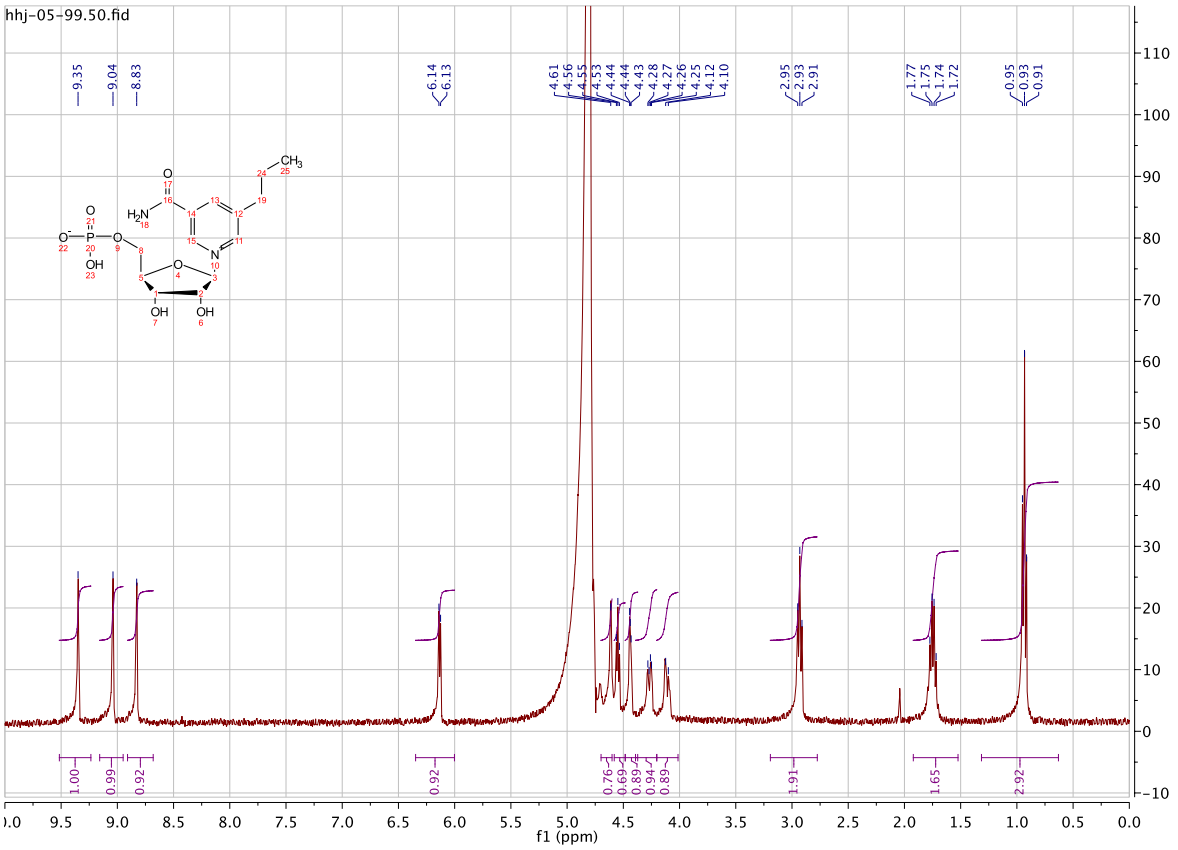
hhj-05-99.50.fid
9.35
9.04
8.83
6.14
6.13
4.61
4.56
4.55
4.53
4.44
4.44
4.43
4.28
4.27
4.26
4.25
4.12
4.10
2.95
2.93
2.91
1.77
1.75
1.74
1.72
0.95
0.93
0.91
1.00
0.99
0.92
0.92
0.76
0.69
0.89
0.94
0.89
1.91
1.65
2.92
f1 (ppm)

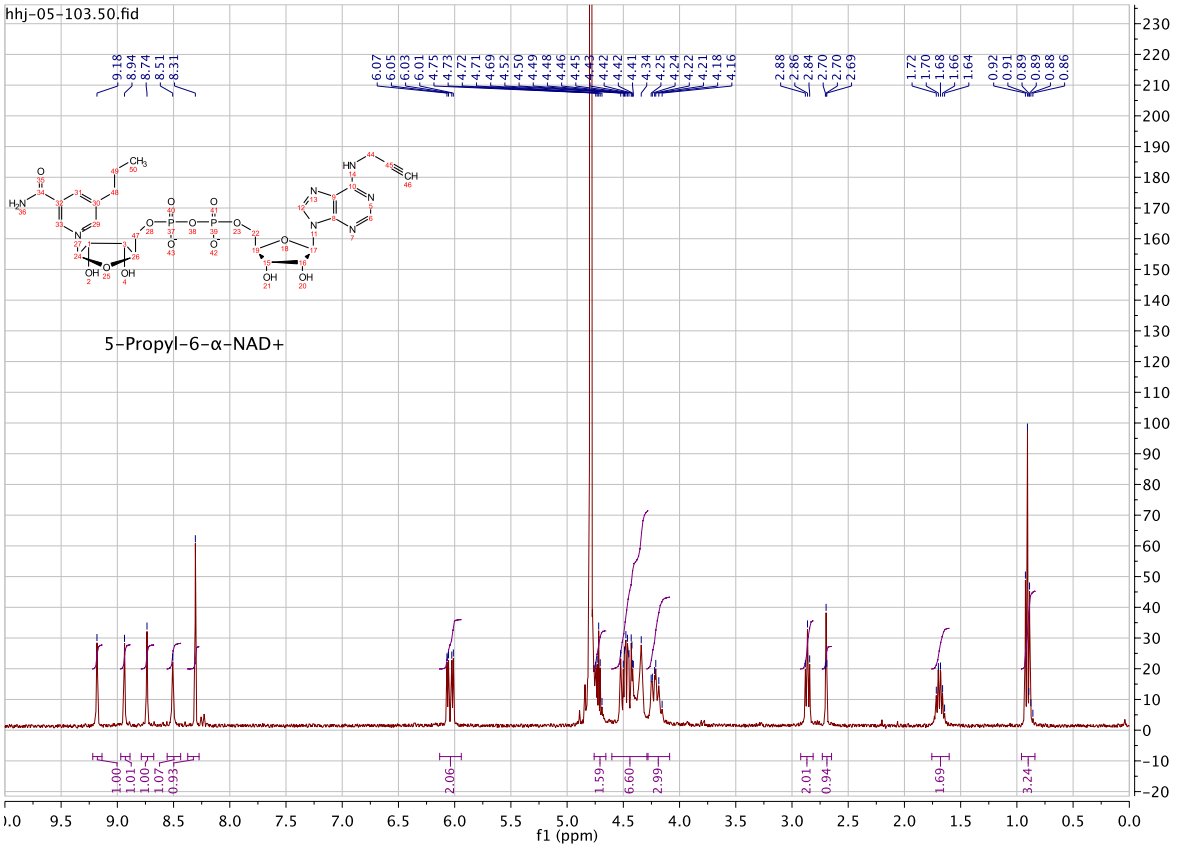
hhj-05-103.50.fid
9.18
8.94
8.74
8.51
8.31
6.07
6.05
6.03
6.01
4.75
4.73
4.72
4.71
4.69
4.52
4.50
4.49
4.48
4.46
4.45
4.43
4.42
4.42
4.41
4.34
4.25
4.24
4.22
4.21
4.18
4.16
2.88
2.86
2.84
2.70
2.70
2.69
1.72
1.70
1.68
1.66
1.64
0.92
0.91
0.89
0.89
0.88
0.86
5-Propyl-6-α-NAD+
1.00
1.01
1.00
1.07
0.93
2.06
1.59
6.60
2.99
2.01
0.94
1.69
3.24
f1 (ppm)

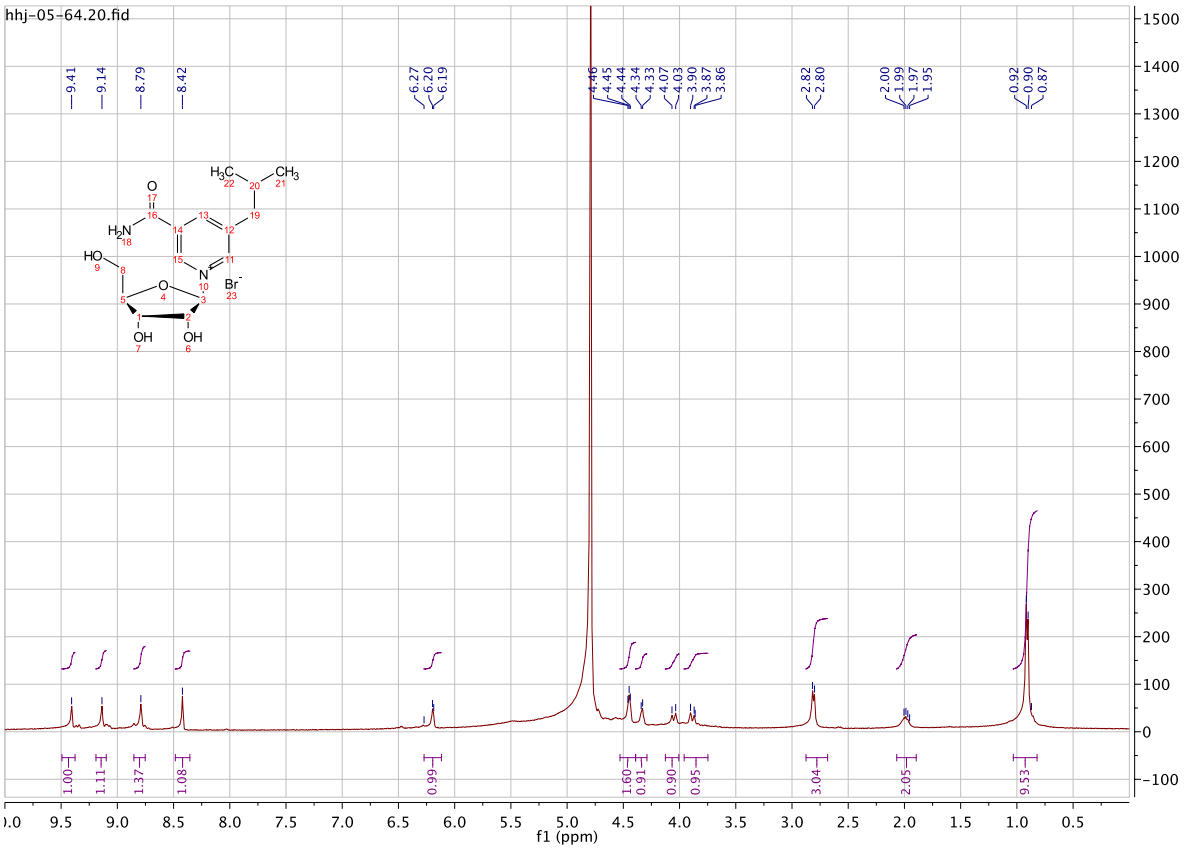
hhj-05-64.20.fid
9.41
9.14
8.79
8.42
6.27
6.20
6.19
4.46
4.45
4.44
4.34
4.33
4.07
4.03
3.90
3.87
3.86
2.82
2.80
2.00
1.99
1.97
1.95
0.92
0.90
0.87
1.00
1.11
1.37
1.08
0.99
1.60
0.91
0.90
0.95
3.04
2.05
9.53
f1 (ppm)


hhj-05-62.1.fid
fr.10-12
9.35
9.01
8.81
8.80
8.80
6.14
6.13
4.61
4.61
4.54
4.52
4.51
4.44
4.43
4.42
4.42
4.29
4.28
4.26
4.26
4.14
4.14
4.13
4.11
4.10
2.84
2.83
2.04
2.02
2.00
1.98
1.97
0.93
0.91
0.91
0.90
1.00
0.88
0.80
0.86
0.95
0.71
0.55
0.75
0.38
1.67
0.75
4.86

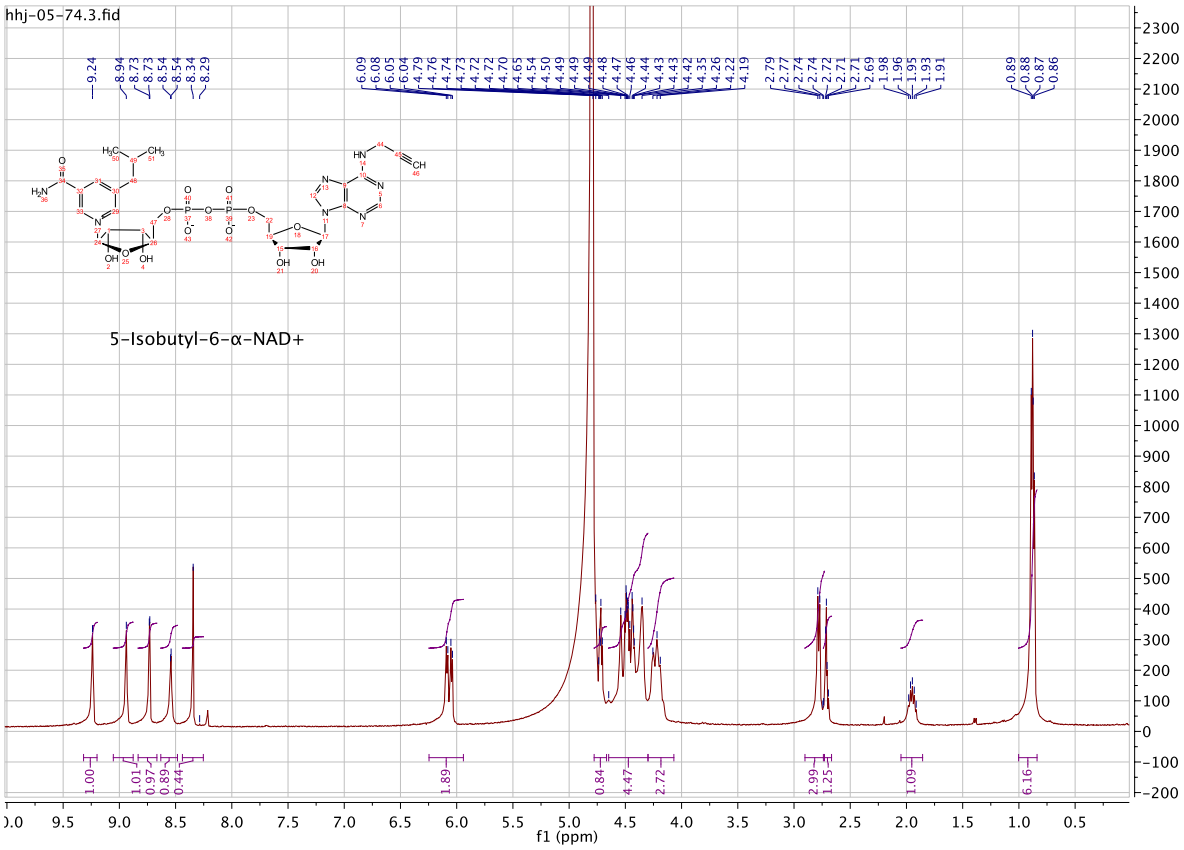
hhj-05-74.3.fid
5-Isobutyl-6-α-NAD+
f1 (ppm)

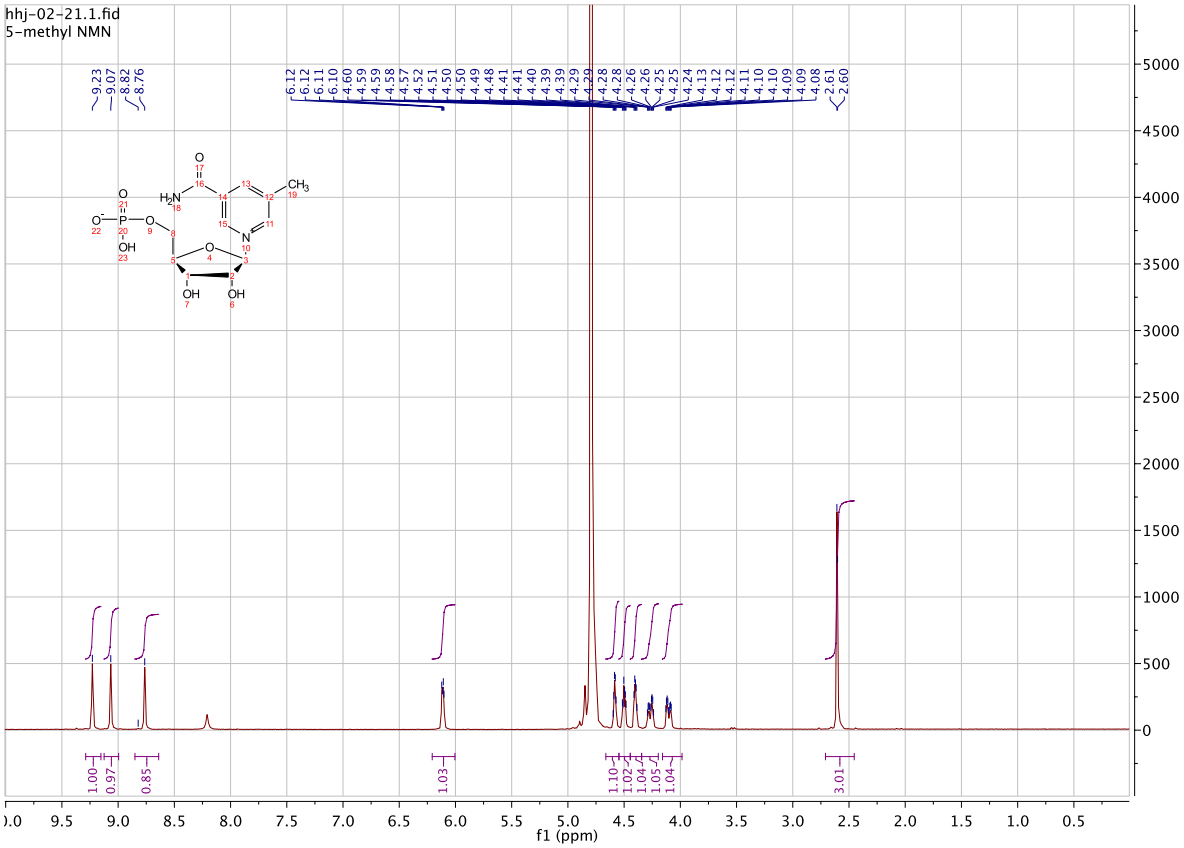
hhj-02-21.1.fid
5-methyl NMN
f1 (ppm)

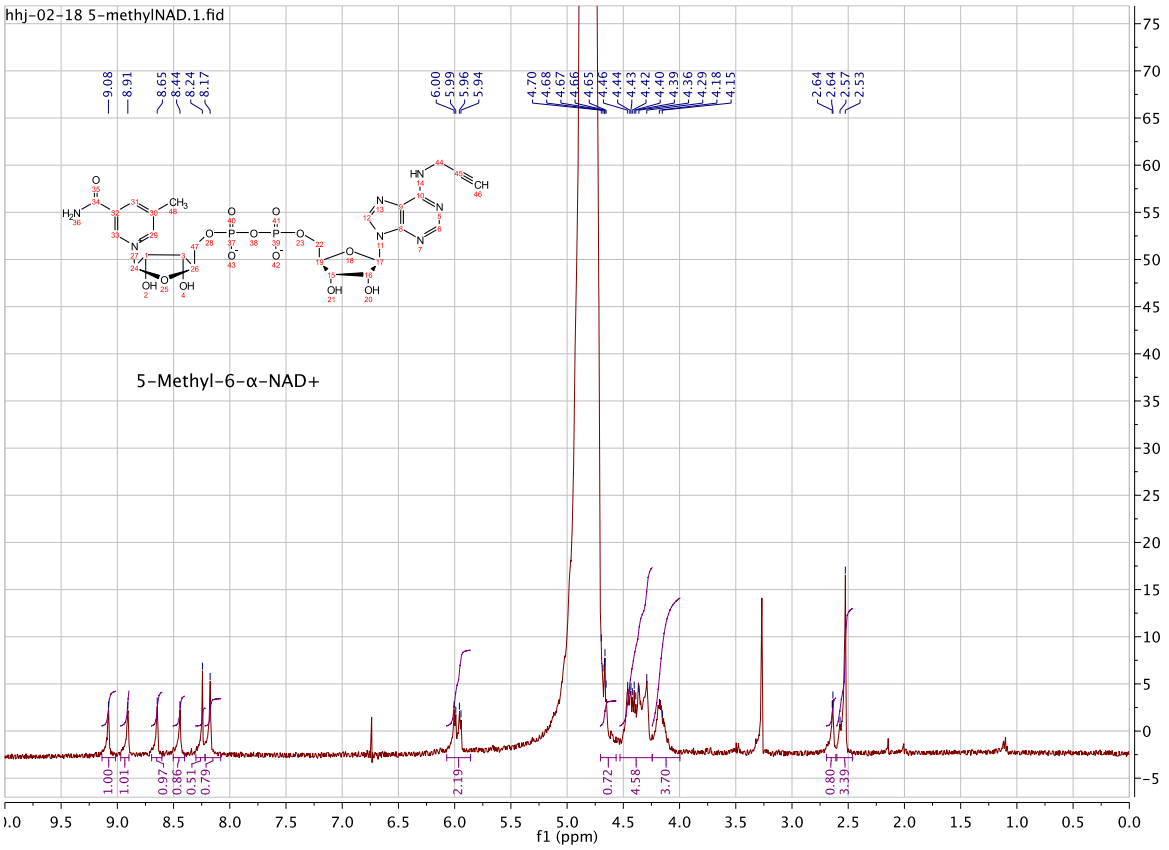

MS/MS Acquisition and Processing. Digests were loaded onto an Acclaim PepMap 0.1 x 20 mm NanoViper C18 peptide trap (Thermo Scientific) for 5 min at a 5 µl/min flow rate in a 2% acetonitrile, 0.1% formic acid mobile phase and peptides separated using a PepMap RSLC C18, 2 µm particle, 75 µm x 25 cm EasySpray column (Thermo Scientific) using a 7.5–30% acetonitrile gradient over 60 min in mobile phase containing 0.1% formic acid and a 300 nl/min flow rate using a Dionex NCS-3500RS UltiMate RSLCnano UPLC system. Tandem mass spectrometry data was collected using an Orbitrap Fusion Tribrid mass spectrometer configured with an EasySpray NanoSource (Thermo Scientific). Survey scans were performed in the Orbitrap mass analyzer at 120,000 resolution, and data-dependent MS2 scans in the linear ion trap using HCD following isolation with the instrument's quadrupole. Full instrument details can be found at www.peptideatlas.org (ID: PASS00764). Raw MS/MS scans were interpreted by SEQUEST using a UniProtKB/Swiss-Prot human database amended with sequences for the GFP-tagged ARTD variants and common contaminants as previously described (Yan et al., 2010). False discovery rate (FDR) for both peptides and proteins was determined through the addition of a complement of sequence-reversed entries from the full search database and discovery of false identifications as previously described (Wilmarth et al., 2009). MARylated ARTD10, ARTD11, and chimeric targets were identified based on the following: (1) at least two unique peptide identifications; (2) total peptide counts enriched ≥ 2-fold above GFP-WT-ARTD controls; (3) and appearance in ≤ half the total background datasets analyzed to date using modified 6-a-NAD^+ probes. Total background datasets can be found at www.peptideatlas.org (ID: PASS00764). GO enrichment was performed using Amigo (Ashburner et al., 2000; Mi et al., 2010; Thomas et al., 2003) – selecting for GO terms enriched with a p-value ≤ 0.05 (unless stated otherwise) – and compression was performed using Revigo (Supek et al., 2011). Confirmation of select MS targets was performed via immunoblot analysis of NeutrAvidin enriched lysate as previously described (Carter-O'Connell et al., 2014). Input controls are shown in Figure S5.

Enzyme Kinetics. SRPK2 and either WT-ARTD10, IG-ARTD10, or WT-ARTD11 were brought up in reaction buffer (50 mM tris-HCl, pH 7.5, 100 mM NaCl, 15 mM $MgCl_2$, and 0.5 mM TCEP) to a final concentration of 1.5 µM (SRPK2) and 500 nM (WT-ARTD10, IG-ARTD10, or WT-ARTD11). 6-a-NAD^+ (for WT-ARTD10 and WT-ARTD11) or 5-Bn-6-a-NAD^+ (for IG-ARTD10) was added at concentrations ranging from 10 – 1000 µM to initiate the MARylation reaction. Equal volume aliquots were removed at 3, 6, 9, and 12 minutes and subjected to click conjugation (100 µM TBTA, 1 mM $CuSO_4$, 100 uM sulforhodamine-N_3, 1 mM TCEP, 1X PBS, and 1% SDS). Click conjugation was halted at 30 minutes with the addition of 2X sample buffer and samples were processed by SDS-PAGE followed by fluorescence detection using the Chemi-Doc (Bio-Rad) system. The fluorescence intensity was quantified in ImageLab (Bio-Rad) and the concentration of ADPr transferred to SRPK2 was determined based on a titration curve using free sulforhodamine-N_3. The initial rates were calculated using Excel (Microsoft) and plotted against the concentration of either 6-a-NAD^+ or 5-Bn-6-a-NAD^+ in Prism (GraphPad). Kinetic parameters were determined using the Michaelis-Menten equation in Prism (GraphPad).

Fluorescence Imaging of GFP-tagged ARTD Variants. HEK 293T cells expressing GFP-tagged variants of WT- or IG-ARTD10, -ARTD11, or Chimera were fixed with paraformaldehyde (4% paraformaldehyde, 4% sucrose, 1X PBS) for 30 min at room temperature. Cover slips were washed in 1X PBS, thrice, and mounted using ProLong Gold (Thermo). Images were captured using an ApoTome microscope (Zeiss) and processed using ImageJ.

SUPPLEMENTAL REFERENCES:

Ashburner, M., Ball, C.A., Blake, J.A., Botstein, D., Butler, H., Cherry, J.M., Davis, A.P., Dolinski, K., Dwight, S.S., Eppig, J.T.*, et al.* (2000). Gene ontology: tool for the unification of biology. The Gene Ontology Consortium. Nature genetics *25*, 25-29.

Mi, H., Dong, Q., Muruganujan, A., Gaudet, P., Lewis, S., and Thomas, P.D. (2010). PANTHER version 7: improved phylogenetic trees, orthologs and collaboration with the Gene Ontology Consortium. Nucleic acids research *38*, D204-210.

Supek, F., Bosnjak, M., Skunca, N., and Smuc, T. (2011). REVIGO summarizes and visualizes long lists of gene ontology terms. PloS one *6*, e21800.

Thomas, P.D., Campbell, M.J., Kejariwal, A., Mi, H., Karlak, B., Daverman, R., Diemer, K., Muruganujan, A., and Narechania, A. (2003). PANTHER: a library of protein families and subfamilies indexed by function. Genome research *13*, 2129-2141.

Wilmarth, P.A., Riviere, M.A., and David, L.L. (2009). Techniques for accurate protein identification in shotgun proteomic studies of human, mouse, bovine, and chicken lenses. Journal of ocular biology, diseases, and informatics *2*, 223-234.

Yan, F.F., Pratt, E.B., Chen, P.C., Wang, F., Skach, W.R., David, L.L., and Shyng, S.L. (2010). Role of Hsp90 in biogenesis of the beta-cell ATP-sensitive potassium channel complex. Molecular biology of the cell *21*, 1945-1954.